Bonding within the Endohedral Fullerenes $Sc_3N@C_{78}$ and $Sc_3N@C_{80}$ as Determined by Density Functional Calculations and Reexamination of the Crystal Structure of $\{Sc_3N@C_{78}\}\cdot Co(OEP)\}\cdot 1.5(C_6H_6)\cdot 0.3(CHCl_3)$

Josep M. Campanera,[‡] Carles Bo,[‡] Marilyn M. Olmstead,[§] Alan L. Balch,*[,§] and Josep M. Poblet*[,‡]

Departament de Química Física i Inorgànica, Universitat Rovira i Virgili, Imperial Tàrraco 1, 43005 Tarragona, Spain, and Department of Chemistry, University of California, Davis, California 95616

Received: August 14, 2002

Density functional calculations have been performed on $Sc_3N@C_{80}$ and $Sc_3N@C_{78}$ to examine the bonding between the scandium atoms and the fullerene cage. The encapsulation of the Sc_3N unit is a strongly exothermic process that is accompanied by a formal transfer of six electrons from the scandium atoms to the fullerene cage in both complexes. In the case of $Sc_3N@C_{78}$, the metal ions are strongly linked to three [6:6] ring junctions of three different pyracylene patches, which are located at the midsection of the fullerene cage. This bonding restricts the Sc_3N unit from freely rotating inside the cage. Geometric optimization of the structure of $Sc_3N@C_{78}$ indicates that the carbon cage expands to accommodate the Sc_3N unit within the cage. This optimized structure has been used to re-refine the crystallographic data for $\{Sc_3N@C_{78}\}\cdot\{Co(OEP)\}\cdot 1.5(C_6H_6)\cdot 0.3(CHCl_3)$. In contrast, in $Sc_3N@C_{80}$, the Sc_3N unit is not trapped in a specific position within the inner surface of the I_h cage, which is an unusual fullerene that lacks pyracylene patches. Thus, free rotation of the Sc_3N group within the C_{80} cage is expected. Despite the electronic transfer from the Sc_3N unit to the carbon cage, $Sc_3N@C_{78}$ and $Sc_3N@C_{80}$ have relatively large electron affinities and ionization potentials.

1. Introduction

The ability of fullerene cages to encapsulate metal ions[1] has been known since the beginning of the fullerene chemistry.[2] Endohedral fullerenes have been found with one, two, or three metal ions (generally group 3 and lanthanide metal ions) inside the carbon cage.[3] In these endohedrals, the carbon cage may be quite small as in $U@C_{28}$[4] or the metal ions may stabilize large clusters such as $La@C_{106}$.[5] The preparations of $Sc_3N@C_{78}$[6] and $Sc_3N@C_{80}$[7] with the planar tetraatomic Sc_3N unit inside the fullerene cage have been reported recently. In the formation of these two clusters, the trimetallic molecule acts as a template, producing $Sc_3N@C_{78}$ and $Sc_3N@C_{80}$, the structures of which are shown in Figure 1, in considerable abundance. However, each of these molecules exhibits a different orientation of the scandium ions with regard to the fullerene cage. Whereas in $Sc_3N@C_{78}$ the metals reside over [6:6] junctions at the center of pyracylene patches, the X-ray characterization for $Sc_3N@C_{80}$[7] and $ErSc_2N@C_{80}$[8] shows that the metals sit over individual carbon atoms in the later and are located near the center of [6:5] bonds in the former. Pyracylene-type sites consist of [6:6] ring junctions abutted by two hexagons (see Figure 2).

There are five isomers for the empty C_{78} cage with symmetries D_3 (78:1), C_{2v} (78:2), $C_{2v'}$ (78:3), D_{3h} (78:4), and $D_{3h'}$ (78:5) that follow the isolated pentagon rule (IPR).[9] Calculations carried out at different levels of theory for these empty cages suggest the following relative stability order: $C_{2v'}$ (78:3) > C_{2v} (78:2) > D_3 (78:1) > $D_{3h'}$ (78:5) > D_{3h} (78:4).[10] Three stable isomers of C_{78} have been separated and their symmetries

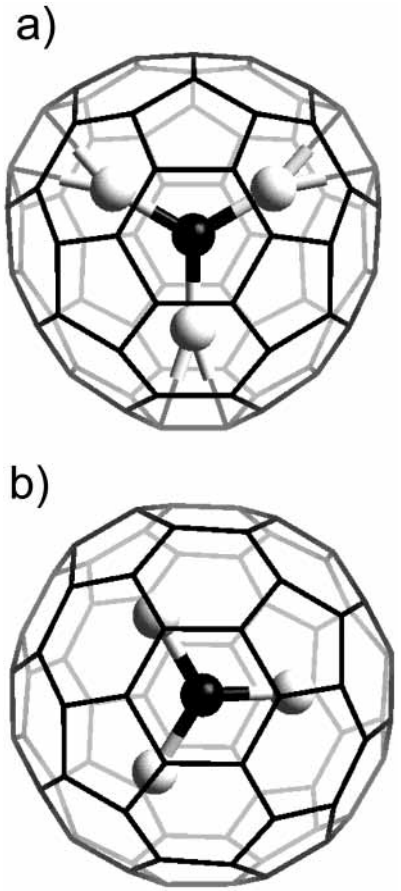

Figure 1. Structures for (a) $Sc_3N@C_{78}$ isomer **1** and (b) $Sc_3N@C_{80}$ isomer **11** for more details see Figures **2** and **6**.

* To whom correspondence should be addressed. E-mail addresses: poblet@quimica.urv.es; albalch@udavis.edu.
‡ Universitat Rovira i Virgili.
§ University of California, Davis.

10.1021/jp021882m CCC: $22.00
Published on Web 11/27/2002

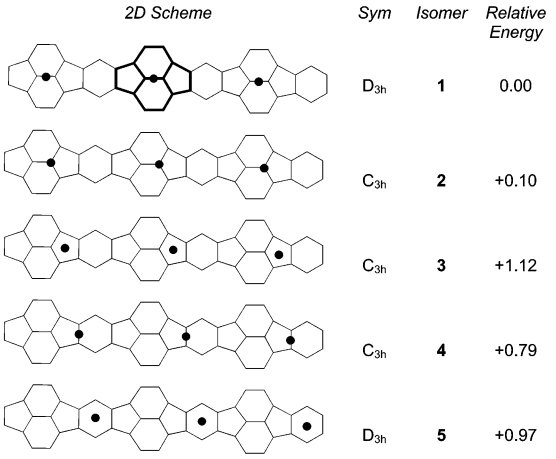

Figure 2. Relative energies (in eV), molecular symmetries, and carbon chains with schematic positions of Sc atoms with respect to the pyracylene patches for the optimized isomers of $Sc_3N@C_{78}$. Bold lines show the pyracylene motif in one of the 2D drawings. In isomer **1** of symmetry D_{3h}, the Sc_3N fragment lies on the σ_h symmetry plane and the scandium atoms (represented by black dots) are over [6:6] ring junctions. The rest of isomers correspond to rotations of the nitride unit keeping the symmetry plane.

identified as $C_{2v'}$ (78:3), C_{2v} (78:2), and D_3 (78:1) through their ^{13}C NMR spectra.[11] The X-ray structure of $Sc_3N@C_{78}$ corresponds, however, to the encapsulation of the nitride moiety by the $D_{3h'}$ (78:5) cage, which is the second least stable empty cage isomer.

Seven isomeric structures of C_{80} with symmetries D_{5d} (80:1), D_2 (80:2), C_{2v} (80:3), D_3 (80:4), $C_{2v'}$ (80:5), D_{5h} (80:6), and I_h (80:7) fulfill the IPR. Two empty cage isomers of C_{80} with D_2 (80:2) and D_{5d} (80:1), symmetries have been isolated.[12] In contrast, in endohedral fullerenes, the cage in $Sc_3N@C_{80}$ has I_h symmetry, and $Ti_2@C_{80}$ has been shown to have D_{5h} symmetry through electron energy loss and ^{13}C NMR spectroscopic studies.[13] Theoretical calculations have shown that, whereas the I_h structure is the least stable isomer for C_{80},[14] the relative stability of this cage increases significantly when six electrons are added to the fullerene.[15] In very recent theoretical work, Kobayashi and co-workers have shown that the I_h form is strongly stabilized by the presence of the template unit, M_3N, inside the cage and that in the series $Sc_{3-n}La_nN@C_{80}$ this stabilization decreases with an increasing number of La atoms.[16]

In this paper, we report a detailed density functional theory (DFT) study of the endohedral clusters $Sc_3N@C_{78}$ and $Sc_3N@C_{80}$ and compare the bonding between the trimetallic nitride unit and the two distinct fullerene cages.

2. Computational and Crystallographic Details

All calculations were carried out using the DFT methodology with the ADF set of programs.[17] We used the local spin density approximation characterized by the electron gas exchange ($X\alpha$ with $\alpha = {}^2/_3$), together with Vosko−Wilk−Nusair[18] (VWN) parametrization for correlation. Becke[19] and Perdew[20] nonlocal corrections were added to the exchange and correlation energy, respectively. Triple-ζ + polarization Slater basis sets were employed to describe the valence electrons of C and N. A frozen core composed of the 1s to 2sp shells for scandium was described by means of single Slater functions. The 3s and 3p electrons were described by double-ζ Slater functions, the *n*d and $(n + 1)$s electrons by triple-ζ functions, and the $(n + 1)$p electrons by a single orbital.[21] Unrestricted calculations were performed for open-shell configurations.

The crystallographic data for $\{Sc_3N@C_{78}\}\cdot\{Co(OEP)\}\cdot 1.5(C_6H_6)\cdot 0.3(CHCl_3)$ were taken from the earlier study and refined by full-matrix least squares based on F^2 (SHELXL-97; Sheldrick, 1998) to yield $wR = 0.268$ for all data; conventional $R1 = 0.098$ computed for 7058 observed data ($>2\sigma(I)$) with 27 restraints and 404 parameters. In comparison, the former refinement gave $R = 0.1175$, $wR = 0.3026$ for all data and conventional $R1 = 0.1107$ computed for 7058 observed data ($>2\sigma(I)$) with 27 restraints and 404 parameters.

3. $Sc_3N@C_{78}$

3.1. The Computed Structure. The $D_{3h'}$ (78:5) isomer is one of the five IPR isomers of C_{78}, and therefore, all C−C bonds involve [6:6] or [6:5] ring junctions. There are several kinds of [6:6] C−C bonds in $D_{3h'}$ (78:5), which range in length from 1.372 to 1.469 Å, and the shortest ones appear in the three pyracylene patches. The [6:5] C−C bonds have an average length of 1.44 Å. These values fall within the range of carbon−carbon distances reported in earlier theoretical studies.[10] There are no X-ray determinations for free C_{78} cages to check the computed geometries, but the present level of computation is capable of reproducing the geometry of C_{60} very well. The computed distances for the two different C−C bonds in C_{60} are 1.398 and 1.453 Å, values that almost coincide with the experimental parameters of 1.401 and 1.458 Å.[22]

Although the free Sc_3N molecule is pyramidal with an optimized Sc−N bond length of 1.957 Å and a Sc−N−Sc bond angle of 99.1°, this fragment has a planar structure inside the fullerene C_{78} and C_{80} cages.[7−8]

A priori, several orientations of the Sc_3N unit inside the fullerene are possible. Because the X-ray determination of $Sc_3N@C_{78}$ shows that the Sc_3N unit lies close to the original σ_h plane of the $D_{3h'}$ (78:5) cage, only isomers that retain this symmetry plane were studied. In the following discussion and in Charts 1 and 2, we consider that the Sc_3N unit is located within the *xy* plane. The σ_h (or *xy*) plane crosses three pyracylene patches that are linked by hexagons as Figure 2 shows. By considering five different orientations of the Sc_3N unit within the C_{78} cage, we computed the five isomers shown in Figure 2. Isomer **1** corresponds to the case in which the scandium atoms are over the [6:6] ring junctions of the pyracylene patches, whereas in isomer **4**, the metals are over [6:5] junctions. In isomer **2**, the metal ions are directly connected to individual carbon atoms. In the other two isomers, each metal is placed at the center of a pentagon (isomer **3**) or a hexagon (isomer **5**).

The full optimization of these five isomers yields five structures with different stability. The relative energies for isomers **1**−**5** are collected in Figure 2. Isomer **1**, with the three Sc atoms bonded to [6:6] ring junctions of pyracylene patches, gives the best orientation for the trimetallic unit inside the cage, an orientation that is 0.79 eV more stable than when the three metals are over the [6:5] ring junctions (isomer **4**). The relative energies of isomers **3** and **5** with respect to **1** are +1.12 and +0.97 eV, respectively. These values clearly indicate that the nitride unit *cannot freely rotate* inside the fullerene cage. However, a rotation of the Sc_3N unit by only 10° in isomer **1** yields structure **2** in which the metals are linked to a unique carbon atom. Because the energy difference between these two isomers is only 0.1 eV, the conversion of **1** to **2** is nearly barrierless. This fact suggests that, although the rotation of the Sc_3N unit is hindered, the structure of the complex may fluctuate dynamically between these two forms.

TABLE 1: Comparison of Some Computed and Experimental Bond Lengths (Å) for Several Isomers of $Sc_3N@C_{78}$ and $Sc_3N@C_{80}$

complex	method	Sc−N[a]	Sc−C[b]	source
		$Sc_3N@C_{78}$		
1	X-ray	1.983−2.125	2.024	ref 6
	X-ray (reexamination)	1.981(6)−2.127(4)	2.206(15)	this work
	DFT-BP	1.997	2.255	this work
		$Sc_3N@C_{80}$		
7	X-ray[c]	1.97−2.06	2.03	ref 8
	DFT-BP	2.004−2.018	2.272	this work
8	DFT-BLYP	2.020−2.029	2.329	ref 16
	DFT-BP	2.008−2.034	2.259	this work
9	DFT-BLYP	2.014−2.029	2.320	ref 16
	DFT-BP	2.010−2.021	2.284	this work
11	X-ray	1.966−2.011	2.170	ref 7
	DFT-BP	2.011−2.021	2.276	this work

[a] Range of Sc−N bond lengths. [b] Contact distances between Sc and the nearest neighbor carbon. [c] Values obtained for $ErSc_2@C_{80}$.

Several attempts have been made to obtain a C_{3v} complex with a pyramidal Sc_3N unit inside the fullerene. However, the optimization process always yielded a geometry with a planar Sc_3N unit.

When a Sc_3N unit is encapsulated by a C_{78} cage to give isomer **1**, there is a significant local distortion in the fullerene cage. This distortion results in the outward movement of the carbon atoms closest to the scandium ions away from these ions. Thus the distortion resembles the distortions seen in exohedral metal complexes of fullerenes, in which bonding to a metal center also results in an outward displacement of the fullerene carbon atoms and increased pyramidalization of the carbon atoms bound to the external metal centers.[23] A similar, but smaller, distortion has also been seen in the chemically modified endohedral $Sc_3N@C_{80}C_{10}H_{10}O_2$.[24] In **1**, the Sc−N bond lengths were found to be 1.997 Å, a close value to the experimental one originally reported for $Sc_3N@C_{78}$ (Table 1). Nevertheless, a major discrepancy appears in the Sc−C bond lengths. Hence, whereas the computed value of 2.255 Å is a common distance for Sc−C bonds, the experimental distances, which range between 2.024 and 2.107 Å in the original refinement with a fixed cage geometry, may be considered very short bond lengths for Sc−C bonds.

3.2. Reexamination of the Crystal Structure of $\{Sc_3N@C_{78}\}\cdot\{Co(OEP)\}\cdot 1.5(C_6H_6)\cdot 0.3(CHCl_3)$. The earlier X-ray crystallographic investigation of the structure of $\{Sc_3N@C_{78}\}\cdot\{Co(OEP)\}\cdot 1.5(C_6H_6)\cdot 0.3(CHCl_3)$ used rigid models for the fullerene cages to distinguish between the five possible IPR isomers for the C_{78} cage and concluded that the $D_{3h'}$ (78:5) cage was present. The resulting model identified three different orientations of the $D_{3h'}$ (78:5) cage and three corresponding orientations of the Sc_3N unit. With that model, the closest Sc−C contacts inside the cage were short (2.024 Å, Table 1) and also quite far from the mean (2.430 Å) and shortest (2.204 Å) Sc−C distances obtained in an exploration of 73 examples in the Cambridge Structural Database.[8] Because of the orientational disorder, free refinement of the cage parameters that might have revealed any structural distortion of the cage by the Sc_3N unit could not be done as part of the original refinement. However, now knowing that the Sc_3N unit does produce a significant change in the dimensions of the C_{78} cage, it is appropriate to reexamine the crystallographic data.

Consequently, the crystallographic data for $\{Sc_3N@C_{78}\}\cdot\{Co(OEP)\}\cdot 1.5(C_6H_6)\cdot 0.3(CHCl_3)$ were re-refined using the optimized computed structure of the C_{78} cage as a new model for the fullerene portion of the structure. Incorporation of this model in the structure into the three locations identified previously and further refinement, in which the orientations of these three groups were allowed to vary, produced a final structure in which the *R* factor decreased from 0.1107 to 0.0977. We consider this reduction in *R* to be significant and conclude that the computed structure is in better agreement with the experimental crystallographic data than was the formerly used rigid cage model. With this model, the Sc−C distances in the major site are Sc1−C37, 2.230(3); Sc1−C38, 2.281(3); Sc2−C6, 2.235(15); Sc2−C7, 2.206(15); Sc3−C66, 2.273(4); and Sc3−C67, 2.239(4) Å. These values are within the range of Sc−C bond lengths found in the Cambridge Structural Database and are consistent with the calculated results reported here. At the major site, the Sc−N distances are Sc1−N, 1.981(6); Sc2−N, 1.967(15); and Sc3−N, 2.127(4). These values are similar to those obtained in the original refinement (Sc1−N, 1.988(7); Sc2−N, 1.983(15); Sc3−N, 2.125(5)).[6] The Sc_3N unit is planar. The sum of the Sc−N−Sc angle is 360°. The individual Sc−N−Sc angles are Sc1−N−Sc2 130.1(5), Sc1−N−Sc3 114.0(2), and Sc2−N−Sc3, 115.9(6).

3.3. The Bonding between the Sc_3N Unit and the Fullerene Cage. The $D_{3h'}$ (78:5) isomer has a closed-shell ground state with three low unoccupied orbitals of symmetries a_2' (−5.15 eV) and e′ (−4.88 eV) that are π antibonding orbitals basically centered in the [6:6] carbon bonds of the pyracylene patches. These unoccupied orbitals can receive six electrons from the three highest occupied orbitals of the trimetallic unit as the orbital interaction diagram of Figure 3 built for isomer **1** shows. The Sc_3N degenerate orbital of symmetry e′ mixes with the lowest unoccupied fullerene orbitals of the same symmetry. The lowest one is the HOMO and is essentially a fullerene orbital as seen in Figure 4. The mixing of orbitals of e′ symmetry leads to a formal transfer of four electrons from the Sc_3N unit to the carbon cage. Orbital a_1' can also interact with C_{78} orbitals, but the lowest a_1' orbital in the empty fullerene is ∼1.8 eV higher than the LUMO, which is of a_2' symmetry. Consequently, there is a transfer of two additional electrons from the metallic orbital of symmetry a_1' to the cage orbital of symmetry a_2'. The a_1' orbital of the Sc_3N fragment becomes the LUMO in the endohedral cluster. In summary, we concluded that formally six electrons are transferred from the nitride unit to the fullerene.

However, the Mulliken populations given in Table 2 suggest that the charge transfer is not so important. The atomic populations for the neutral nitride indicate that this molecule is a polar molecule with a strong negative charge localized on N (−1.14 e) and a positive charge on each Sc of +0.38 e. Taking as reference the planar form of Sc_3N, the encapsulation by C_{78} induces a lowering of 1.08 electrons in the s orbitals in each Sc. However, the populations of p and d orbitals increase by 0.18 and in 0.48 e, respectively, and the total charge of each Sc atom in the endohedral is +0.88 e. The charge on the Sc atom in the endohedral is positive but far from +2.59 e, the positive charge of the metal ion in a free Sc_3N^{6+} unit. Notice in values of Table 2 that despite the transfer of charge between the neutral nitride and the fullerene, the nitrogen atom increases its negative charge up to −1.41 e. Globally, there is a charge transfer between the two units of 1.23 e.

The analysis of the electron density difference (EDD) maps is a useful tool to characterize chemical bonds in large molecules.[25] An important property of the EDD maps is that they are less dependent on the basis set than the Mulliken populations. Figure 5 contains contour lines in the σ_h plane associated with accumulations and depletions of charge density when the electron density of $ScN_3@C_{78}$ is computed with respect

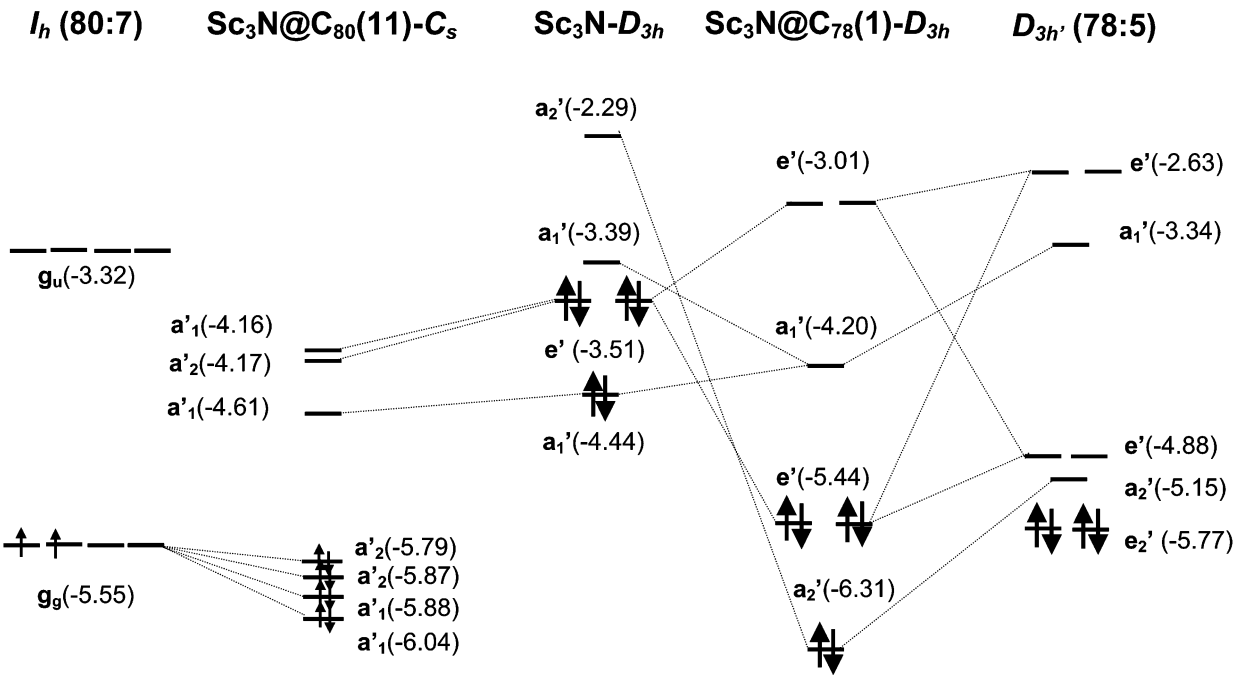

Figure 3. Orbital interaction diagram for $Sc_3N@C_{78}$ (isomer **1**) and $Sc_3N@C_{80}$ (isomer **11**). Only the most important orbitals that participate in the bonding have been drawn. The isolated icosahedral C_{80} has the open-shell configuration $...(t_{1g} + h_u)^{16}(g_g)^2(h_g + a_g)^0...$, meanwhile the $D_{3h'}$ isomer of C_{78} has the closed-shell configuration $...(e_2)^4(a'_2)^0...$.

TABLE 2: Mulliken Populations for the Sc_3N Unit in Several Molecules

		Sc				N			
molecule	sym	net charge	s	p	d	net charge	s	p	d
Sc_3N[a]	C_{3v}	+0.38	1.00	6.23	1.39	−1.14	1.85	4.27	0.02
Sc_3N[b]	D_{3h}	+0.46	1.20	6.21	1.13	−1.38	1.84	4.53	0.01
Sc_3N^{6+}[b]	D_{3h}	+2.59	0.00	5.93	0.48	−1.77	1.90	4.86	0.01
$Sc_3N@C_{78}$ (**1**)[a]	D_{3h}	+0.88	0.12	6.39	1.61	−1.41	1.83	4.57	0.01
$Sc_3N@C_{80}$ (**11**)[a]	C_s	+0.86	0.15	6.43	1.56	−1.44	1.84	4.59	0.01

[a] Optimized structure. [b] Planar structure with Sc−N distance from distance found in $Sc_3N@C_{78}$ isomer **1**.

its subunits Sc_3N and C_{78}. The electronic density exhibits accumulations close to carbon atoms directly bonded to Sc atoms that may be associated with electronic transfers from Sc_3N to the π_{C-C}* orbitals. The accumulations near the Sc atoms show that there is a reorganization in the Sc orbitals, which shows that 3d orbitals take an active part in the formation of the cluster. This reorganization is fully consistent with the Mulliken populations. Roszak and Balasubramanian investigated the metal−ligand bond in the simple molecule ScC_2 and concluded that the interaction between Sc and the C_2 unit is highly ionic with a strong transference to the C−C sigma bond that does not occur in the present case.[26]

The bonding between the C_{78} cage and the Sc_3N unit is also analyzed using the extended transition method developed by Ziegler and Rouk[27] that is an extension of the well-known decomposition scheme of Morokuma.[28] According to this method, the bonding energy (BE) between two fragments can be decomposed into several contributions:

$$\mathrm{BE} = (\Delta E_{\mathrm{DE}} + \Delta E_{\mathrm{ST}} + \Delta E_{\mathrm{ORB}})$$

ΔE_{DE} is the deformation energy term, that is, the energy necessary to convert the fragments from their equilibrium to the geometry in the cluster. ΔE_{ST} is the steric interaction term and represents the interaction energy between the two deformed fragments with the electron densities that each fragment would have in the absence of the other fragment. This term has two contributions, the Pauli repulsion and the classical electrostatic interaction. Finally, the orbital interaction term (ΔE_{ORB}) represents the stabilization produced when the electron densities are allowed to relax and accounts for the charge transfer between fragments and the mutual polarization of each fragment. The sum $\Delta E_{\mathrm{ST}} + \Delta E_{\mathrm{ORB}}$ is known as the fragment interaction energy and represented by ΔE_{INT}. Recently, Sgamellotti and co-workers have used this method to rationalize the metal−fullerene bonding in organometallic derivatives of C_{60}.[29]

The encapsulation process of the trimetallic unit into a C_{78} cage is a strongly exothermic process that yields a binding energy of −9.70 eV for isomer **1**. Decomposition of the BE energy with respect its components is given in Table 3. A free Sc_3N unit has a pyramidal geometry in which the Sc−N bond distance was computed to be 1.957 Å at the present level of theory. The ΔE_{DE} necessary for Sc_3N to achieve the planar structure with a Sc−N distance of 1.997 Å, the optimal distance in isomer **1**, is 0.72 eV, whereas 1.49 eV is the ΔE_{DE} that the fullerene cage requires to accommodate the Sc_3N unit in its interior. The interaction between the two fragments amounts −11.91 eV, a term that is dominated by the orbital contribution ($\Delta E_{\mathrm{ORB}} = -35.3$ eV). The other component to ΔE_{INT} is the steric repulsion that was found to be very positive, $\Delta E_{\mathrm{ST}} = +23.4$ eV. The large value computed for the orbitallic term corroborates that when two neutral fragments are put together there is an important electronic reorganization as we have seen through the orbital diagram in Figure 3 and the EDD map in Figure 5.

The formal transfer of six electrons between the two moieties makes also convenient the analysis of the BE energy with respect to the ionic fragments $[Sc_3N^{6+}]$ and $[C_{78}^{6-}]$ (Table 3). The interaction energy between these two fragments to give **1** is −136.6 eV, a large energy difference, which is dominated by the classical electrostatic interaction between the two highly charged ions. The electrostatic interaction is much larger than

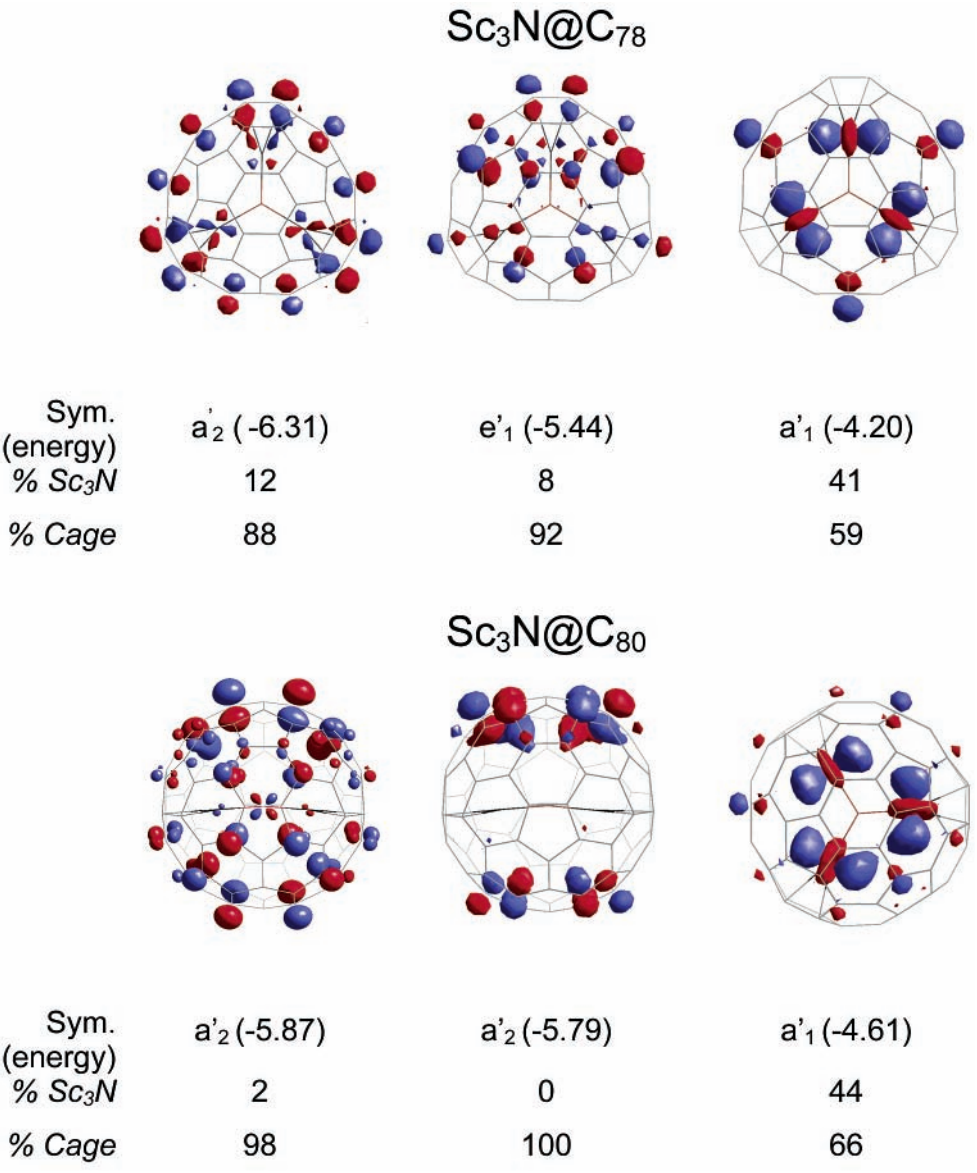

Figure 4. Symmetries, 3D representations, energies (in eV), and composition of the most important orbitals involved in charge transfer and bonding for the optimized complexes of $Sc_3N@C_{78}$ (isomer **1**) and $Sc_3N@C_{80}$ (isomer **11**).

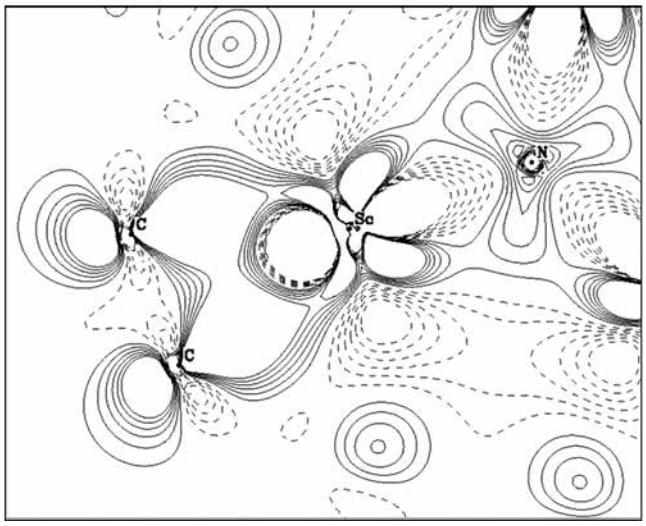

Figure 5. Electron density difference map (EDDM) for $Sc_3N@C_{78}$ (isomer **1**). The electron density that has been computed as the difference ρ(endohedral) − [ρ(nitride) + ρ(cage)] is represented in a plane containing Sc_3N and two carbon atoms.

TABLE 3: Decomposition of the Binding Energy (BE) for All Optimal Isomers of $Sc_3N@C_{78}$ (Isomers 1−5) and the Most Stable Isomer of $Sc_3N@C_{80}$ (Isomer 11)

				ΔE_{DE}[a] (eV)		
complex	ΔE_{ST} (eV)	ΔE_{ORB} (eV)	ΔE_{INT} (eV)	Sc_3N	cage	BE[b] (eV)
			$Sc_3N@C_{78}$			
1	23.43	−35.34	−11.91	0.72	1.49	-9.70
1[c]	−81.62	−54.98	−136.60		0.72	
2	22.88	−34.54	−11.66	0.67	1.37	−9.62
3	21.60	−31.86	−10.26	0.62	1.05	−8.59
4	21.76	−32.69	−10.93	0.62	1.38	−8.93
5	21.47	−32.15	−10.68	0.65	1.29	−8.74
			$Sc_3N@C_{80}$			
11	20.07	−3.04	−12.97	0.79	0.58	−11.60

[a] Deformation energy (ΔE_{DE}) is the energy necessary to modify the fragment from its optimal geometry to the structure that it has in the endohedral cluster. [b] BE = $\Delta E_{DE} + \Delta E_{INT}$. [c] Decomposition of the BE with respect to the ionic fragments Sc_3N^{6+} and C_{78}^{6-}. The deformation energy for the Sc_3N unit was not determined because we were unable to find a minimum for the cation.

the Pauli repulsion. Consequently, the steric term, that is, the sum of these two terms, is very negative; $\Delta E_{ST} = -81.62$ eV.

TABLE 4: Decomposition of the Interaction Energy (ΔE_{INT}) for Several Model Complexes of $Sc_3N@C_{78}$

isomer	ΔE_{ST}[a] (eV)	ΔE_{ORB}[b] (eV)	ΔE_{INT}[c] (eV)
1	26.76	−34.91	−8.15
2	26.58	−34.69	−8.11
3	26.42	−33.82	−7.40
4	26.85	−34.02	−7.17
5	25.69	−33.18	−7.49

[a] Steric energy (ΔE_{ST}) includes Pauli repulsion and classical electrostatic interaction. [b] The orbital interaction term (ΔE_{ORB}) accounts for the stabilization produced when fragment orbitals of each subunit, Sc_3N and C_{78}, mix for giving the endohedral cluster. [c] Fragment interaction energy ($\Delta E_{INT} = \Delta E_{ST} + \Delta E_{ORB}$) is the resulting stabilizing energy associated with the interaction between the planar Sc_3N (d_{Sc-N} = 1.975 Å) and C_{78} at its optimal free geometry.

These two large energies are totally consistent with the high charge located on each fragment. Nevertheless, the very large contribution to the stabilizing energy associated with the orbital term is unexpected. The ΔE_{ORB} term was found to be −54.98 eV, value that is even larger than the corresponding term when the fragments are neutral. After the encapsulation of [Sc_3N^{6+}] by [C_{78}^{6-}], there is an important *orbital mixing* and consequently an important electronic reorganization that induces a transfer of charge (in this case from the anionic cage to the cationic nitride) and a polarization of each unit. Both fragment polarization and charge transfer occur simultaneously, and unfortunately, they are not easy to separate. In the ionic decomposition, the ΔE_{DE} term is almost negligible in comparison to ΔE_{INT}.

Table 3 also contains the decomposition energy terms of the BE for isomers **2**−**5**. The values for isomer **2** are very similar to those of isomer **1** because both structures are very close. For the other three isomers, **3**−**5**, the repulsive steric term and the stabilizing orbitallic term are smaller in magnitude than those in **1** but the decrease is larger in the orbitallic term. Consequently, ΔE_{INT} is less stabilizing when the scandium ions are focusing other sites than those close to carbons that form [6:6] ring junctions. In other words, when the Sc ions are over [6:6] C−C bonds, the mixing of orbitals between the two fragments is maximized. Nevertheless, the *intrinsic* electronic and steric properties of the different fullerene sites are better understood if fixed fragment geometries are used in the energy decomposition analysis. This process allows us to isolate the changes in ΔE_{INT} from the effects due to changes in the geometry of the fragments. This procedure has been effective in identifying ligand donor and acceptor properties in organometallic complexes.[30] We have studied the interaction between a planar Sc_3N unit with the Sc−N distance equal to 1.975 Å—an intermediate value between 1.966 and 1.983 Å, the most frequently observed Sc−N bond lengths in these endohedral clusters—and a carbon cage with the geometry of the free fullerene. Using these unrelaxed fragments, we have searched the best orientation of a fixed planar Sc_3N unit in a rigid C_{78} cage for the five orientations described in Figure 2. Roughly, the relative energies obtained with the unrelaxed structures (Table 4) are quite similar to those found for the optimized clusters (Figures 2). Notice that in these model structures the deformation energy is only due to the Sc_3N fragment and has the same value for all orientations. This contribution has not been included in Table 4. Because of the similar environment that scandium ion has in **1** and **4**, the steric term is not very different in these two isomers. Therefore, the greater stabilization when Sc ions reside over a [6:6] bond arises from the orbital contribution. The larger contribution of the ΔE_{ORB} term to ΔE_{INT} in **1** may be attributed to the effective overlap between the cage orbitals of symmetries e′ and a_2' and the Sc d_{xy}-type orbitals (see Chart 1). This overlap

CHART 1: In-Plane Bonding Interaction between Metal and [6:6] Carbon Bond in $Sc_3N@C_{78}$ (Isomer 1)

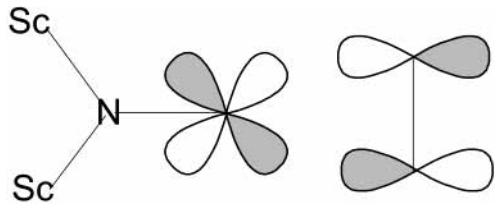

CHART 2 Nonbonding Interaction between Metal and [6:5] Carbon Bond in $Sc_3N@C_{78}$ (Isomer 4)

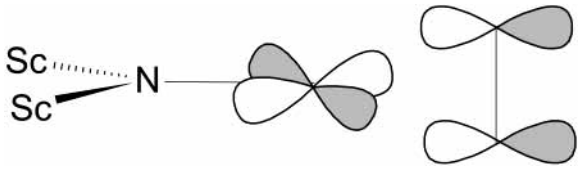

does not occur when Sc atoms reside over [6:5] bonds, as in isomer **4**, because the e′ and a_2' cage orbitals in the [6:5] ring junction regions are perpendicular to the Sc_3N plane (Chart 2). When the Sc ions are placed at the center of a pentagon (isomer **3**) or a hexagon (isomer **5**), the ΔE_{ST} and ΔE_{ORB} terms are smaller in absolute values than those in **1** because the Sc−C distances are larger. The longer Sc−C distances create less-effective fragment orbital overlap but smaller steric repulsions. The loss of overlap effectiveness is greater than the diminution of the steric repulsion. Consequently, ΔE_{INT} in **3** and **4** is smaller than that in **1**. In other words, when the scandium orbitals, localized in the symmetry plane, interact with the cage orbitals there is a gradual stabilization of the interacting cage orbitals. This effect reaches a maximum in isomer **1**. In summary, the analysis on the model structures clearly shows that Sc_3N is trapped in specific position due to an *orbital* effect.

4. $Sc_3N@C_{80}$

The Sc_3N unit strongly stabilizes the icosahedral isomer of C_{80}, which is the most unstable of the seven structures that satisfy the isolated pentagon rule for empty cage C_{80}. Previous theoretical calculations have shown that the I_h isomer has the open-shell configuration ...$(t_{1g} + h_u)^{16}(g_g)^2(h_g + a_g)^0$.... Moreover, I_h (80:7) may deform to lower symmetries by Jahn−Teller effect.[31] In the case of $Sc_3N@C_{80}$, there is evidence from the ^{13}C NMR spectrum that the trimetallic nitride may freely rotate inside the cage.[7] Following the same strategy used for C_{78}, we have studied several orientations of the trimetallic unit inside the fullerene. The orientations considered have always maintained one plane of symmetry in the endohedral. Figure 6 shows the six structures that we have considered. In three of them (**6**−**8**), the molecular plane of the Sc_3N unit coincides with the symmetry plane of the endohedral cluster. In the other three orientations (**9**−**11**), the plane of symmetry contains the N atom and one of the Sc atoms; the symmetry plane relates the other two Sc's.[32] With these six isomers, we have tried to cover a large number of the alternatives for where the metals can be found inside the icosahedral isomer of C_{80}. In structure **6**, the three metals are directed toward the center of two pentagons and one hexagon. Isomers **7** and **8** represent slight rotations of the trimetallic unit in relation to **6**, whereas in **11** the three metal ions are oriented toward [6:5] ring junctions, and finally structures **9** and **10** correspond to a slight change in relation to **11**. Indeed, this latter structure was computed to be the most stable and coincides with the X-ray structure observed for

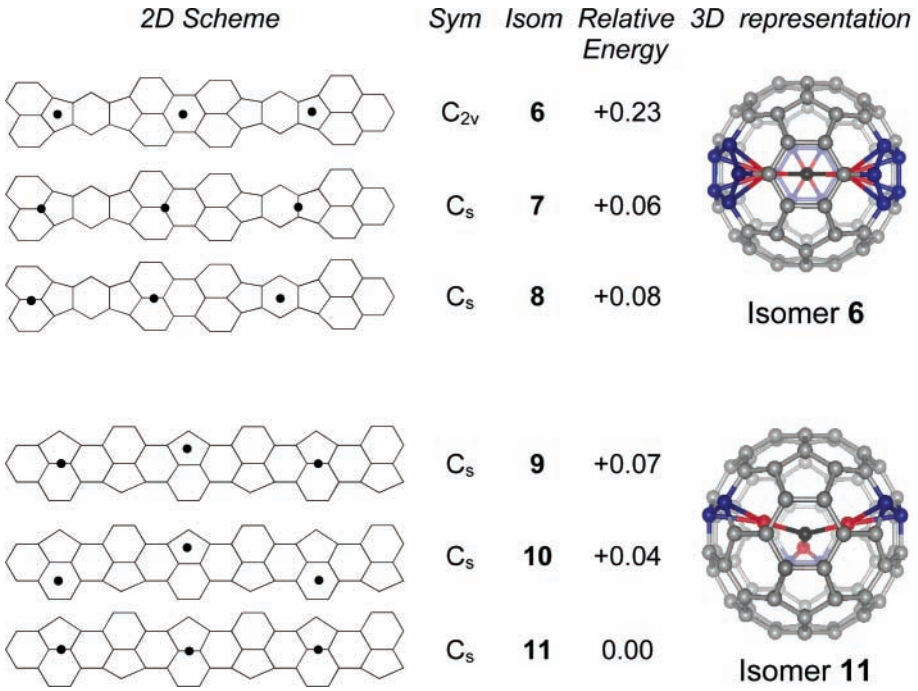

Figure 6. Relative energies (in eV), symmetries, and carbon chains with schematic position of Sc atoms in a 2D representation for the optimized isomers of $Sc_3N@C_{80}$. The 3D representation for isomers **6** (C_{2v}) and **11** (C_s) shows the connections between the metal ions and carbons. In isomer **6**, the Sc_3N unit lies on one of the symmetry planes that retains the endohedral. Isomers **7** and **8** are simply rotations of the metallic nitride with respect **6**. Clusters **9**, **10,** and **11** have also C_s symmetry, but in these isomers, the symmetry plane contains the nitrogen atom and one of the metals. Like those in Figure 2, the relative position of scandiums with respect to the cage is represented by black dots in the 2D scheme.

$Sc_3N@C_{80}$.[7] The geometry found for $ErSc_2N@C_{80}$[8] is better represented by isomer **7**. Like those in the endohedral of C_{78}, the theoretical Sc−C distances for $Sc_3N@C_{80}$ are longer than the experimental ones but the differences are smaller. On the other hand, our structures for isomers **8** and **9** almost coincide with those found by Kobayashi and co-workers using the BLYP functional (Table 1).[16]

For $Sc_3N@C_{80}$, the energy difference between the distinct isomers is rather small, <2 kcal mol^{-1} for the majority of the Sc_3N orientations (Figure 6). Only in isomer **6**, in which the three ions are oriented toward the center of three polygons, is the relative energy of the cluster is somewhat higher, ∼5.3 kcal mol^{-1} with respect to **11**. These relative energies for the $Sc_3N@C_{80}$ isomers yield the conclusion that the Sc_3N unit may easily rotate inside the fullerene cage. As in C_{78}, the encapsulation of Sc_3N into the I_h isomer of C_{80} results in a formal transfer of six electrons from the scandium atoms to the fullerene orbitals. As a consequence of this electron transfer, the resulting endohedral has a closed-shell configuration (Figure 3). Mulliken population analysis given in Table 2 shows that the electronic population on the nitride unit and the charge transfer between the two moieties are almost identical to those found for $Sc_3N@C_{78}$. The incorporation of Sc_3N into the I_h isomer of C_{80} is, however, somewhat more exothermic than in the case of formation of $Sc_3N@C_{78}$ because the binding energy was found to be approximately 1.9 eV more stabilizing. The energetic difference between these two encapsulation processes essentially arises from the larger Sc−C bond distances in the larger fullerene (see Table 1). Two factors contribute to the lengthening of Sc−C bond when going from C_{78} to C_{80}: a moderate increase of the cage radius[33] from 4.05 to 4.10 Å and the different framework of these two cages. The direct consequence is that the steric repulsion (ΔE_{ST}) is less destabilizing in $Sc_3N@C_{80}$, and this lower steric repulsion is accompanied by a minor deformation energy on going from the empty cage to the endohedral geometry (Table 3). The orbital interaction term (ΔE_{ORB}) is also very important but somewhat minor in the C_{80} cluster when it is compared with the most stable endohedral of C_{78}. Notice from the orbital interaction diagram in Figure 3 and orbital composition in Figure 4 that the quadruply degenerate g_g orbitals of the I_h isomer of C_{80} are less stabilized than the corresponding frontier orbitals in C_{78} because of *lower mixing* with the Sc orbitals. The greater binding energy in the larger cluster may be associated with the smaller steric repulsion between the two fragments and the lower energy necessary to deform the larger fullerene (Table 3). The binding energy for $Sc_3N@C_{80}$ was computed to be −11.6 eV (−267 kcal mol^{-1}), a value that is quite similar to the energy reported very recently by Kobayashi and co-workers who studied the energetics of isomers **8** and **9** using the B3LYP functional.[16] From the small energy difference found between structures **8** and **9**, Kobayashi and co-workers also concluded that Sc_3N is free to rotate inside the fullerene.

5. Physical Properties of $Sc_3N@C_{78}$ and $Sc_3N@C_{80}$

Calculations were also carried out to compute the vertical electron affinity (EA) and ionization potential (IP) of these two endohedrals. Fullerenes, in general, exhibit relatively large EAs, behavior that is related to the presence of low-lying unoccupied orbitals. In particular, Smalley and co-workers estimated from photoelectron spectra an EA of ca. 2.60−2.80 eV for C_{60}.[34] In the gas phase, C_{60} can accept two electrons giving rise to the C_{60}^{-2} ion. In solution, electrochemical studies have shown that C_{60} can be easily reduced to form the ions C_{60}^{-n} ($n = 1-6$). At the present level of theory, the adiabatic and vertical EAs for C_{60} were computed to be 2.88 and 2.85 eV, values that are in excellent agreement with the experimental data.[35] The isolated $D_{3h'}$ (78:5) and I_h (80:7) clusters have larger vertical electron affinities, 3.49 and 3.75 eV, respectively, because of their very low-lying unoccupied orbitals. The formal transfer of six electrons from the Sc_3N unit to the cage reduces the EA of these

TABLE 5: Computed Vertical Ionization Potentials (IP) and Electron Affinities (EA) for Several Optimized Molecules (in eV)

molecule	sym	IP	EA	*E*(HOMO)	*E*(LUMO)
Sc_3N	C_{3v}	5.05	1.27	−3.21	−2.92
C_{60}	I_h	7.57	2.85	−6.25	−4.59
C_{78}	$D_{3h'}$	6.88	3.49	−5.77	−5.15
C_{80}	I_h	6.92	3.75	−5.55	−3.32
$Sc_3N@C_{78}$ (**1**)	D_{3h}	6.53	2.55	−5.44	−4.20
$Sc_3N@C_{80}$ (**11**)	C_s	6.88	2.99	−5.79	−4.61

two fullerenes to 2.55 and 2.99 eV. This latter computed energy completely agrees with the estimated value of 2.81 ± 0.05 eV measured by Ioffe et al. for $Sc_3N@C_{80}$.[36] To our knowledge, no electron affinity determination has been reported for $Sc_3N@C_{78}$. The relatively large electron affinities computed for $Sc_3N@C_{80}$ and $Sc_3N@C_{78}$ suggest that these compounds, like C_{60}, should be easily reducible. It is important to notice from values of Table 5 that the EAs of the endohedrals are not compared to the EA of the most stable isomer of each empty-cage fullerene. Another interesting feature is that these two endohedrals exhibit moderately large HOMO−LUMO gaps, a fact that explains their relative stability and abundance. The HOMOs in $Sc_3N@C_{80}$ and $Sc_3N@C_{78}$ are somewhat less stabilized than are the HOMOs in C_{60}. Therefore, these endohedrals exhibit IPs that are slightly smaller than that of C_{60}.

6. Conclusions

DFT calculations carried out on $Sc_3N@C_{78}$ clearly suggest that the encapsulation of a Sc_3N unit inside the $D_{3h'}$ (78:5) cage is accompanied by an important degree of charge transfer from the trimetallic unit to the carbon cage that induces a high degree of stabilization for both units. The binding energy for this process was computed to be −9.7 eV (−224 kcal mol^{-1}), a rather large stabilization energy. In the endohedral $Sc_3N@C_{78}$ the Sc ions are strongly linked to [6:6] ring junctions of pyracylene patches. This bonding does not allow the Sc_3N unit to freely rotate inside the fullerene. Steric repulsion forces the C_2 units closest to the Sc ions to be pushed away from the fullerene surface, a feature that the original X-ray characterization of $Sc_3N@C_{78}$ did not show.[6] However, reexamination of the crystallographic data using the structure computed here for $Sc_3N@C_{78}$ shows that this model provides a better fit to the data than the rigid C_{78} cage employed previously. Although, $Sc_3N@C_{78}$ may be *formally* described by the ionic model $[Sc_3N]^{6+}-[C_{78}]^{6-}$ the difference of 26 kcal mol^{-1} between the most and least stable isomers is basically due to an *orbital* effect.

In essence, the bonding between the Sc_3N unit and the icosahedral isomer of C_{80} is comparable to the analogous union in C_{78}, but the lack of any pyracylene regions in I_h (80:7) makes the two endohedrals ($Sc_3N@C_{78}$ and $Sc_3N@C_{80}$) different. In the latter, the scandium ions are not trapped in a specific position of the fullerene. The binding energy is somewhat greater in the larger cluster, a fact that may be attributed to the smaller steric repulsion. Despite the formal charge transfer of six electrons from the Sc_3N unit to the carbon cage, these two endohedrals have relatively large electron affinities, which suggests that their redox properties should be similar to those of C_{60}.

Acknowledgment. All calculations have been carried out on workstations purchased with funds provided by the DGICYT of the Government of Spain and by the CIRIT of Generalitat of Catalunya (Grant Nos. PB98-0916-C02-02 and SGR01-00315). A.L.B. thanks the U. S. National Science Foundation for support (Grant CHE 0070291). We thank the referees for comments and suggestions.

Supporting Information Available: X-ray crystallographic data collection and structure refinement, tables and atomic coordinates, bond distances and angles, anisotropic thermal parameters, and hydrogen atom positions for $\{Sc_3N@C_{78}\}\cdot\{Co(OEP)\}\cdot 1.5(C_6H_6)\cdot 0.3(CHCl_3)$ in CIF format. This information is available free of charge via the Internet at http://pubs.acs.org.

References and Notes

(1) Heath, J. R.; O'Brien, S. C.; Zhang, Q.; Liu, Y.; Curl, R. F.; Kroto, H. W.; Tittel, F. K.; Smalley, R. E. *J. Am. Chem. Soc.* **1985**, *107*, 7779.

(2) Kroto, H. W.; Heath, J. R.; O'Brien, S. C.; Curl, R. F., Smalley, R. E. *Nature* **1985**, *318*, 162.

(3) See, for example, the reviews: (a) Shinodora, H. In *Fullerenes*: *Chemistry, Physics and Technology*; Kadish, K. M., Ruoff, R. S., Eds.; John Wiley and Sons: New York, 2000; p 237. (b) Nagase, S.; Kobayashi, K.; Akasaka, T.; Wakahara, T. In *Fullerenes*: *Chemistry, Physics and Technology*; Kadish, K. M., Ruoff, R. S., Eds.; John Wiley and Sons: New York, 2000; p 395. (c) Nagase, S.; Kobayashi, K.; Akasaka, T. *Bull. Chem. Soc. Jpn*. **1996**, *69*, 2131.

(4) Guo, T.; Diener, M. D.; Chai, Y.; Alford, M. J.; Haufler, R. E.; McClure, S. M.; Ohno, T.; Weaver, J. H.; Scuseria, G. E.; Smalley, R. E. *Science* **1992**, *257*, 1661.

(5) Alvarez, M. M.; Gillan, E. G:; Holcker, K.; Kaner, R. B.; Min, K. S.; Whetten, R. L. *J. Phys. Chem.* **1991**, *95*, 10561.

(6) Olmstead, M. M.; Bettencourt-Dias, A.; Duchamp J. C:; Stevenson, S.; Marciu, D.; Dorn, H. C.; Balch, A. L. *Angew. Chem., Int. Ed.* **2001**, *40*, 1223.

(7) Stevenson, S.; Rice, G.; Glass, T.; Harich, K.; Cromer, F.; Jordan, M. R.; Craft, J.; Hadju, E.; Bible, R.; Olmstead, M. M.; Maltra, K.; Fisher, A. J.; Balch, A. L.; Dorn, H. C. *Nature* **1999**, *401*, 55.

(8) Olmstead, M. M.; Bettencourt-Dias, A.; Duchamp, J. C.; Stevenson, S.; Dorn, H. C.; Balch, A. L. *J. Am. Chem. Soc.* **2000**, *122*, 12220.

(9) Fowler, P. W.; Manoloupoulus, D. E. *An Atlas of Fullerenes*; Oxford University Press: Oxford, U.K., 1995; p 254.

(10) Zhang, B. L.; Wang, C. Z.; Ho, K. M. *Chem. Phys. Lett.* **1992**, *193*, 225. Slanina, Z.; Francois, J.-P.; Bakowies, D.; Thiel, W. *J. Mol. Struct. (THEOCHEM)* **1993**, *279*, 213. Bühl, M.; van Wüllen, C. *Chem. Phys. Lett.* **1995**, 247, 63. Osawa, E.; Ueno, H.; Yoshida, M.; Slanina, Z.; Zhao, X.; Nishiyama, M.; Saito, H. *J. Chem. Soc., Perkin Trans 2* **1998**, 943. Sun, G.; Kertesz, M. *J. Phys. Chem. A* **2000**, *104*, 7398. Heine, T.; Seifert, G.; Fowler, P. W.; Zerbetto, F. *J. Phys. Chem.* **1999**, *103*, 8738.

(11) Diederich, F.; Whetten, R. L.; Thielgen, C.; Ettl, R.; Chao, I.; Alvarez, M. M. *Science* **1991**, *254*, 1768. Kikuchi, K.; Nakahara, N.; Wakabayashi, T.; Suzuki, S.; Shiromaru, H.; Miyake, Y.; Saito, K.; Ikemoto, I.; Kainosho, M.; Achiba, Y. *Nature* **1992**, *357*, 142. Taylor, R.; Langley, J. G.; Dennis, T. J. S.; Kroto, H. W.; Walton, D. R. M. *J. Chem. Soc., Chem. Commun.* **1992**, 1043.

(12) Hennrich, F. H.; Michel, R. H.; Fischer, A.; Richard-Schneider, S.; Gilb, S.; Kappes, M. M.; Fuchs, D.; Bürk, M.; Kobayashi, K.; Nagase, S. *Angew. Chem., Int. Ed. Engl.* **1996**, *35*, 1732. Wang, C.-R.; Sugai, T.; Kai, T.; Tomiyama, T.; Shinohara, H. *Chem. Commun.* **2000**, 557.

(13) Cao, B.; Hasegawa, M.; Okada, K.; Tomiyama, T.; Okazaki, T.; Suenaga, K.; Shinohara, H. *J. Am. Chem. Soc.* **2001**, *123*, 9679.

(14) Kobayashi, K.; Nagase, S.; Akasaka, T. *Chem. Phys. Lett.* **1995**, *245*, 230.

(15) Fowler, P. W.; Zerbetto, F. *Chem. Phys. Lett.* **1986**, *131*, 144.

(16) Kobayashi, K.; Sano, Y.; Nagase, S. *J. Comput. Chem.* **2001**, *22*, 1353.

(17) *ADF 2.3 User's Guide*; Chemistry Department, Vrije Universiteit: Amsterdam, The Netherlands, 1997. Baerends, E. J.; Ellis, D. E.; Ros, P. *Chem. Phys.* **1973**, *2*, 41. Fonseca Guerra, C.; Visser, O.: Snijders, J. G.; te Velde, G.; Baerends, E. J. In *Methods and Techniques in Computational Chemistry*: *METECC-95*; Clementi, E., Corongiu, G., Eds.; STEF: Cagliari, Italy, 1995; p 305.

(18) Vosko, S. H.; Wilk, L.; Nusair, M. *Can. J. Phys.* **1980**, *58*, 1200.

(19) Becke, A. D. *J. Chem. Phys.* **1986**, 84, 4524; *Phys. Rev.* **1988**, *A38*, 3098.

(20) Perdew, J. P. *Phys. Rev.* **1986**, *84*, 4524; **1986**, *B34*, 7406.

(21) Snijders, J. G.; Baerends, E. J.; Vernooijs, P. *At. Data Nucl. Data Tables* **1982**, *26*, 483. Vernooijs, P.; Snijders, J. G.; Baerends, E. J. *Slater type basis functions for the whole periodic system*; Internal Report; Free University of Amsterdam: Amsterdam, The Netherlands, 1981.

(22) Hedberg, K.; Hedberg, L.; Bethune, D. S.; Brown, C. A.; Dorn, H. C.; Johnson, R. D.; de Vries, M. *Science* **1991**, *254*, 410.

(23) Balch, A.; Olmstead, M. M. *Chem. Rev.* **1998**, *98*, 2123.

(24) Lee, H. M.; Olmstead, M. M.; Iezzi, E.; Duchamp, J. C.; Dorn, H. C.; Balch, A. L. *J. Am. Chem. Soc.* **2002**, *124*, 3494.

(25) *Electron Distributions and the Chemical Bond*; Coppens, P., Hall, M. B., Eds.; Plenum Press: New York, 1981.

(26) Roszak, S.; Balasubramanian, K. *J. Phys. Chem. A* **1997**, *101*, 2666−2669. Benard, M.; Rohmer, M.-M.; Poblet, J. M. *Chem. Rev.* **2000**, *100*, 495. Li, X.; Wang, L.-S. *J. Chem. Phys.* **1999**, *111*, 8389.

(27) Ziegler, T.; Rauk, A. *Theor. Chim. Acta* **1977**, *46*, 1−10. Ziegler, T.; Rauk, A. *Inorg. Chem.* **1979**, *18*, 1558−1565.

(28) Morokuma, K. *J. Chem. Phys.* **1971**, *55*, 1236−1244. Kitaura, K.; Morokuma, K. *Int. J. Quantum Chem.* **1976**, *10*, 325−340.

(29) Nunzi, F.; Sgamelloti, A.; Re, N.; Floriani, C. *Organometallics* **2000**, *19*, 1628.

(30) Gonzalez-Blanco, O.; Branchadell, V. *Organometallics* **1997**, *16*, 5556.

(31) Lee, S. L.; Sun, M. L.; Slanina, Z. *Int. J. Quantum Chem.* **1996**, *60*, 355.

(32) In structures **6**−**11**, the four atoms of the Sc_3N fragment are not strictly coplanar but the deviation from the planarity is very small.

(33) Cage radius is defined as the average distance of all carbons to the center of the fullerene.

(34) Yang, S. H.; Pettiette, C. L.; Conceicao, J.; Cheshnowsky, O.; Smalley, R. E. *Chem. Phys. Lett.* **1987**, *139*, 233.

(35) Brink, C.; Andersen, L. H.; Hvelplund, P.; Mathur, D.; Voldstad, J. D. *Chem. Phys. Lett.* **1995**, *233*, 52.

(36) Ioffe, I. N.; Boltalina, O. V.; Sidorov, L. N.; Dorn, H. C.; Stevenson, S.; Rice, G. In *Fullerenes*: *Recent Advances in the Chemistry and Physics of Fullerenes and Related Materials*; Kadish, K. M., Ruoff, R. S., Eds.; Electrochemical Society: Pennington, NJ, 2000; p 166.